

Magnetic Properties of the Intermediate State in Small Type-I Superconductors

Alexander D. Hernandez and Daniel Domínguez
 Centro Atómico Bariloche and Instituto Balseiro,
 8400 San Carlos de Bariloche, Río Negro, Argentina.

We present simulations of the intermediate state of type-I superconducting films solving the time dependent Ginzburg-Landau equations, which include the demagnetizing fields via the Biot-Savart law. For small square samples we find that, when slowly increasing the applied magnetic field H_a , there is a saw-tooth behavior of the magnetization and very geometric patterns, due to the influence of surface barriers; while when slowly decreasing H_a , there is a positive magnetization and symmetry-breaking structures. When random initial conditions are considered, we obtain droplet and labyrinthine striped patterns, depending on H_a .

PACS numbers: 74.25.-q, 74.25.Ha, 75.60.-d

In 1937 Landau modeled the intermediate state (IS) in thin slabs of type-I superconductors, assuming a periodic structure of alternating stripes of normal and superconducting phases.¹ Direct experimental observation of the IS revealed that, while in some cases its structure resembled the Landau picture, very complex patterns and history dependence were usually seen.^{2,3,4,5} Similar type of complex structures were later observed in two-dimensional (2D) systems where there is a competition among interfacial tension and long-range interactions⁶ like thin magnetic films, ferromagnetic fluids, Langmuir and lipid monolayers, and self-assembled atoms on solid surfaces.⁶ Labyrinthine patterns, and a transition from structures of droplets to stripes are typically observed.⁶ The rich physics found in these 2D systems has motivated a renewed interest in the study of the IS in type-I superconductors in several recent experiments.^{7,8,9,10,11}

Most of the theoretical progress^{12,13,14,15,16,17,18,19,20} has been made by modeling the IS with periodic arrays of normal and superconducting phases. Recently, a current-loop model¹⁸ which allows to describe simple non periodic patterns has been introduced, but a fully consistent theoretical description¹⁹ of the experimental patterns is still needed. Another important problem not addressed neither experimentally nor theoretically in type-I superconductors is the study of the IS in samples of sizes comparable with the expected periodicity of the patterns, while interesting "mesoscopic" behaviors have been found in type-II superconductors with sizes of the order of few times the magnetic size (λ) of vortices.²¹

In this paper we report detailed simulations of small square type-I superconductors by solving the time dependent Ginzburg-Landau (TDGL) equations for slabs of thickness d . We consider the "non-branching case", where $d \leq \lambda_s \approx 800(\text{\AA})$,¹³ which can be well approximated by reducing the equations to a 2D problem, as done for example in Ref.12,18. We therefore assume that the current density J and the order parameter can be replaced by their average over z for $d/2 < z < d/2$, i.e. $J(R; z) \rightarrow J(R)$ and $\psi(R; z) \rightarrow \psi(R)$, with $R = (x, y)$ the in-plane coordinate. The TDGL equations,^{17,18} in

the gauge where the electrostatic potential is zero, are

$$\frac{\partial}{\partial t} = \frac{1}{\epsilon_0} \nabla^2 \psi - \frac{2e}{\hbar c} \mathbf{r} \cdot \frac{2e}{\hbar c} \mathbf{A} \quad (1)$$

$$\mathbf{J} = \frac{1}{8\pi e^2} \nabla \times \left(\frac{2e}{\hbar c} \mathbf{A} \right) - \frac{n}{c} \frac{\partial \mathbf{A}}{\partial t} \quad (2)$$

Here \mathbf{r} , \mathbf{A} , \mathbf{J} are 2D in-plane vectors, $\epsilon_0 = \kappa^2 D$, D is the diffusion constant, n the normal state conductivity, λ the penetration depth and ξ the coherence length. These 2D approximated TDGL equations couple with the perpendicular component of \mathbf{B} . Following Ref.22 we express the z -averaged sheet current \mathbf{J} by a scalar function g : $\mathbf{J}(R) = \nabla g(R)$. This guarantees that $\nabla \cdot \mathbf{J} = 0$, the physical meaning of $g(R)$ being the local magnetization or density of tiny current loops. Next one relates $g(R)$ with $B_z(r) = \nabla \cdot \mathbf{A}$ at $z = 0$ and the applied field H_a by means of the Biot-Savart law:²²

$$B_z(R; z=0) = H_a + \frac{1}{c} \int \nabla^2 Q(R; R') g(R') d^2 R' \quad (3)$$

The kernel Q satisfies $Q(R_1; R_2) = Q(R_2; R_1)$; $\nabla^2 Q(R) = -\delta(R)$; and $\nabla^2 R Q(R) = 0$ (due to ux conservation). To a good approximation the kernel can be given by (see K. Maki in Ref. 12): $Q(R) = \frac{1}{4} \ln(R) = \frac{1}{4} [\ln(R^2 + d^2/4)]^{1/2}$. The boundary conditions are $(\nabla g)_b = 0$ and $g_b = 0$. We solve the equations with a finite difference scheme with discretization $x = y = 0.5(0)$, using link variables to maintain the gauge invariance.¹⁷ We normalize time by $t_0 = \frac{4\pi\epsilon_0\hbar^2}{n^2 c^2}$, A by $H_{c2}(0)(0)$, T (temperature) by T_c , and take $\epsilon_0 = t_0 = 12$. To obtain $g(R)$ we invert (3) using the conjugate gradient method as done in Ref.23.

We show results for square samples of size $L \times L$ with $L = 256(0)$, thickness $d = 40(0)$; $\kappa = 1.5$; $T = 0.8T_c$ and time step $\tau = 0.25$ (we also obtained similar results for $L = 120(0) \times 256(0)$, $d = 10(0) \times 40(0)$ and $\kappa = 0.4 \times 0.6$). We performed simulations of the intermediate state following three different procedures: (i) slowly increasing the magnetic field from $H_a = 0$, (ii) slowly decreasing the magnetic field from the normal state ($H_a > H_c$) and (iii) starting from random initial

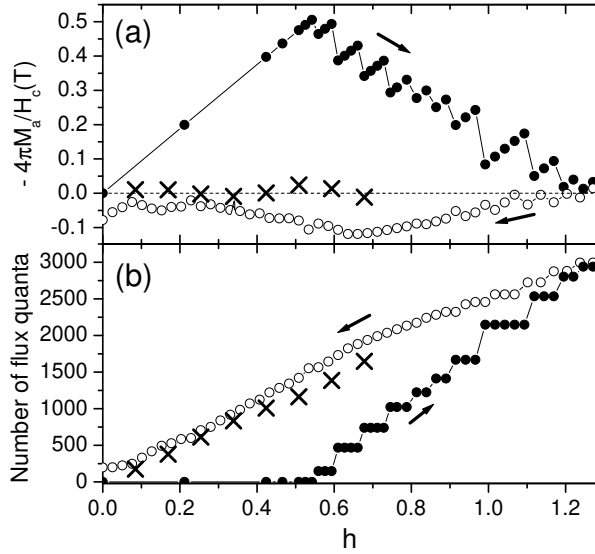


FIG. 1: (a) $(B_z - H_a) = H_c(T)$ and (b) the number of flux quanta obtained increasing (closed circles), decreasing (open circles) the external magnetic field $h = H_a = H_c(T)$, and with random initial conditions (crosses).

conditions for each value of H_a . The global results for the three cases are summarized in Fig. 1. We show the apparent magnetization, $4\pi M_a = h B_z - H_a$ (real magnetization is $4\pi M = B_z - H$, but M_a is what can be determined experimentally), in Fig. 1 (a), and the number of flux quanta inside the sample, $N_{\phi} = \int (A + \frac{J_s}{j}) dl$, in Fig. 1 (b), as a function of $h = H_a = H_c(T)$.

(i) Slowly increasing the magnetic field. We start from $H_a = 0$ with a state with $j(R)j^2 = 1$ and $B_z(R) = 0$ and increase H_a in small steps, after reaching a stationary state for each field (when $jE = E_j < 10^{-6}$; where E is the change in energy between consecutive time steps). We observe a Meissner state for $H_a < H_p = 0.56 H_c$. Surface barriers preclude the penetration of flux below H_p . The surface barrier in macroscopic type-I superconductors can lead to relatively large first penetration fields H_p , which depend on the sample shape and dimensions.^{7,15} Here the smallness of our system strongly enhances this effect. We observe that at $H \approx H_p$ four long chunks of the normal phase, carrying hundreds of flux quanta, enter from each side of the square and equilibrate in the pattern shown in Fig. 2 (a). At a higher field H_{p2} , some other four chunks of flux enter and form the pattern seen in Fig. 2 (b). Further increasing the field, more complex structures form, as shown in Fig. 2 (c) and (d). The normal domains tend to stay in the centre of the sample, leaving a flux-free zone near the edge. Above H_c , flux has fully entered inside the system and there is only surface superconductivity until $H_{c3} > H_c$. The internal structure of the domains is detailed in Figs. 2 (e) and 2 (f) which show transversal cuts of $j(R)j^2$ and $B_z(R)$ taken at the center of one of the faces for $h = 0.58$. In Fig. 2 (e) we see that in the normal regions there is a

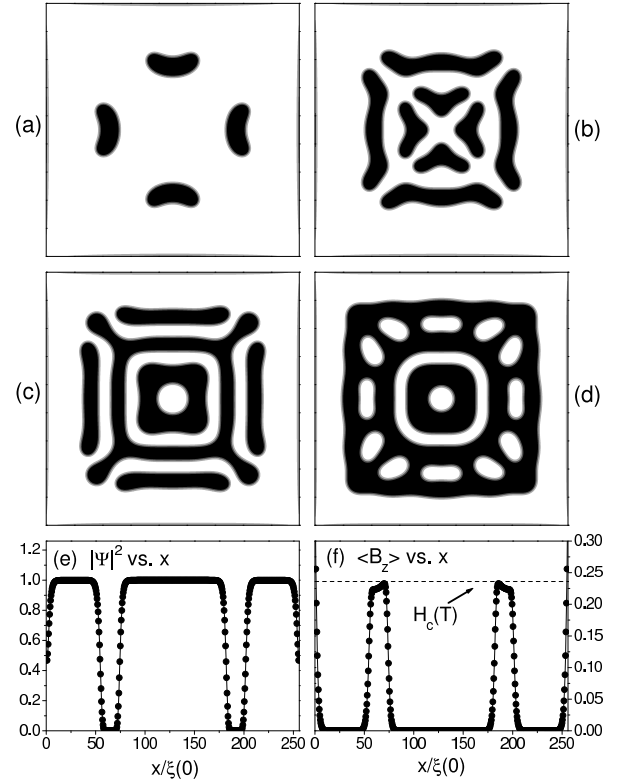


FIG. 2: (a)–(d) Spatial patterns of $j(r)j^2$ obtained continuously increasing $h = H_a = H_c$ from $h = 0$. (a) $h = 0.58$, (b) $h = 0.65$, (c) $h = 0.72$ and (d) $h = 0.78$. Gray scale ranging from black for $j(r)j^2 = 0$ to white for $j(r)j^2 = 1$. (e) and (f) show transversal cuts of $j(r)j^2$ and hB_z taken at the center of one of the faces for $h = 0.58$ (Fig. 2 (a)). Parameters: $\kappa = 0.6$, $d = 40$ (0) and sample size 256 (0) $\times 256$ (0).

sharp drop to zero of $j j^2$ and that $B_z = H_c(T)$ (see Fig. 2 (f)). The global structure of the patterns of the IS observed in Figs. 2 (a)–(d) follow the geometry of the sample and have the symmetry of the square. In general, we find that the entrance of the normal phase occurs only for discrete values of penetration fields $H_{p,i}$ where several flux quanta are nucleated at the four sides of the square, while for $H_{p,i} < H_a < H_{p,i+1}$, there is no flux entrance. This shows up as a saw-tooth behavior in the magnetization in Fig. 1 (a) and as a series of plateaus and jumps in the number of flux quanta vs. H_a in Fig. 1 (b). This type of behavior is similar to the results observed in mesoscopic type-II system²¹ which also show a saw-tooth behavior of the magnetization. However, while in Ref. 21 each jump in M_a corresponds to the entrance of one quantum of flux (one vortex), here at each jump in M_a several hundreds of flux quanta have entered. Our results suggest the existence of a "mesoscopic-like" behavior in small type-I samples. This novel behavior appears when the linear size L of the sample only allows for a small number of normal domains inside the system. This means that L is not more than one order of magnitude

larger than the periodicity of the patterns at intermediate fields. Indeed, we have found similar "mesoscopic-like" behavior for sizes in the range $L \approx 256$ (0).

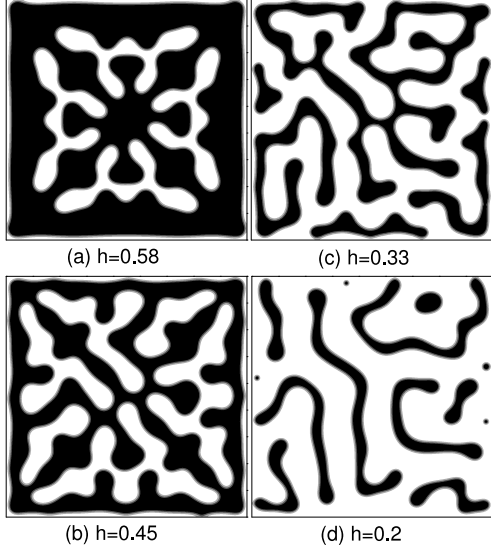


FIG. 3: Spatial patterns of $j(r)j^2$ obtained decreasing h from the normal state at $h = 1$. Same parameters as in Fig. 2.

(ii) Slowly decreasing the magnetic field. We start from $H_a > H_c$ with a state with $\phi = 0$ and $B = H_a$ and decrease H_a in small steps, after reaching a stationary state for each field. The resulting intermediate state patterns are shown in Fig. 3. When $H_a = H_c$ the superconducting phase enters into the sample and the total number of flux quanta is reduced. At first, the superconducting phase forms four chunks embedded within the normal phase, which nearly follow the square symmetry of the system, as shown in Fig. 3 (a). However, we observe that when decreasing the field the square symmetry is always broken in the patterns. The breaking of symmetry is stronger the further we decrease the field. In this way, labyrinthine patterns are formed at mid-range fields, as can be seen in Figs. 3 (b) and (c). In general, the expulsion of flux occurs gradually when decreasing H_a as shown in Fig. 1 (b). For low fields we see that thin stripes of normal phase are trapped within the sample, as shown in Fig. 3 (d). The difficulty for expelling flux is due to the surface barrier and results in a positive magnetization as a function of h as shown in Fig. 1 (a). Even at $h = 0$, a small amount of flux remains trapped in the sample, as evidenced in Fig. 1 (b), where the number of flux quanta is finite at $h = 0$, and in Fig. 1 (a), where $M_a > 0$ at $h = 0$. In experiments in macroscopic samples it has been observed that some trapped flux remains in the system at $h = 0$ when decreasing the field³ and in some Sn-In samples a positive magnetization has been obtained when decreasing H_a .⁵ It is interesting to mention that a similar positive magnetization was observed in mesoscopic type-II superconductors²¹ when decreasing H_a , and attributed to the importance of surface barriers.

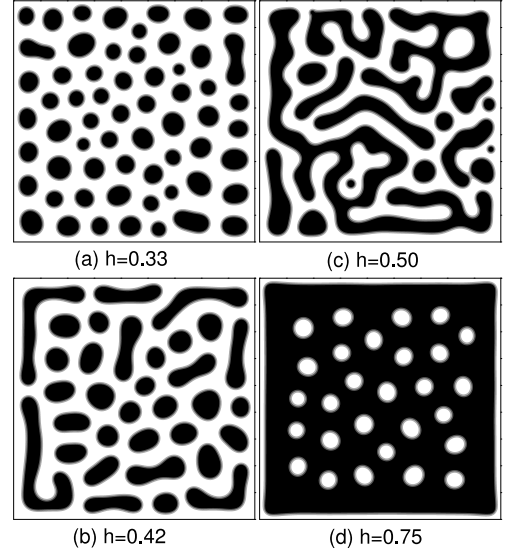


FIG. 4: $j(r)j^2$ patterns obtained using random initial conditions. Same parameters as in Fig. 2.

(iii) Random initial conditions. The structures of the IS discussed above, obtained either increasing or decreasing the magnetic field, are strongly influenced by the surface barriers and/or the geometry of the small sample simulated. In a film of large linear size L the demagnetization factor N is such that $1 \leq N \leq d/L \ll 0$, and therefore we expect that $B = H_a$. To obtain stationary states more typical of the bulk behavior of large samples, we start with a initial condition with random values of A and ϕ , such that we satisfy $\langle B \rangle = H_a$ from the start, and that the initial state is superconducting in average, $\langle j^2 \rangle > 0$. We performed simulations with this initial condition for different values of h , and let the system to evolve for each case, using a stronger criterion for assuming stationarity: $\langle j^2 \rangle = \langle j^2 \rangle < 10^{-9}$. We obtain that in the stationary state most of the flux remains inside the sample and $\langle B \rangle = H_a \approx 0$ as can be seen in Fig. 1 (a). The structures obtained are shown in Fig. 4. For low fields, we observe in Fig. 4 (a) that the intermediate state consists of almost circular droplets of the normal phase. For higher fields, the droplets start to coalesce into long lamellar-like domains, as seen in Fig. 4 (b). At intermediate fields, as shown in Figs. 4 (c), labyrinthine patterns of stripes of the normal phase are formed. For high fields close to H_c we observe almost circular droplets of the superconducting phase embedded within the mostly normal phase, see Fig. 4 (d). Similar type of structures, with droplets of one or the other phase at low and high fields, and with labyrinthine patterns of stripes at mid range fields has been observed experimentally for example in Figs. 2.8 (a)–(f) of Ref. 2 for a lead thin film. An important feature we find in our small system is that there is a thin layer of superconducting phase at the surface (see Fig. 4), which allows for the screening Meissner currents.

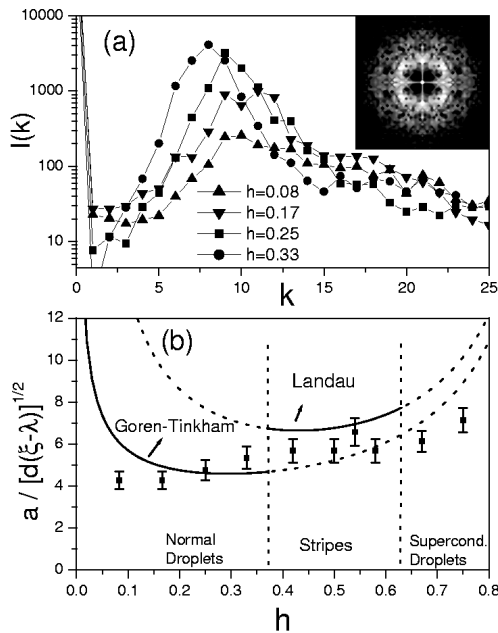


FIG. 5: (a) Spectral intensities obtained from $j(x)j^2$ at different magnetic fields, a maximum at k_0 is observed. The inset shows the Fourier transform of Fig. 4(a). (b) Periodicity $a = 2\pi/k_0$ of each structure as a function of h . The lines correspond to the Landau and the Goren-Tinkham models.

We analyze the structures obtained in Fig. 4, by calculating the spectral transform of the superconducting order parameter, $I(k) = \int dr j(x)j^2 \exp(ik \cdot r)$, which is shown in Fig. 5(a). The non-periodicity and complex

structure of the patterns results in very broad maxima in $I(k)$ at finite wave vectors $k_0 = 2\pi/a$ which define a typical length scale a . In the case of low and large fields, a would correspond to the typical distance between droplets, while for mid-range fields, a would correspond to the average widths of the stripes in the labyrinthine patterns. We plot a in Fig. 5(b) and compare it with the Landau model of stripes¹ and with a model of Goren and Tinkham for a periodic array of droplets or "flux spots".¹⁴ We see that the Landau model agrees qualitatively with the results obtained at mid-range h (for these fields the patterns of Fig. 4 can have a mixture of "stripes" with a few droplets, which make a smaller than the Landau value). On the other hand, at low h the Goren-Tinkham model does not agree well with the size of the droplets obtained. Also in some experiments^{4,10} it has been found a departure from the Goren-Tinkham model at low fields.

In conclusion, our simulations predict that the strong influence of the surface barriers in small type-I samples will lead to a saw-tooth behavior of the magnetization and very geometric patterns when slowly increasing H_a , and to a positive magnetization and symmetry-breaking structures when slowly decreasing H_a . These results suggest the existence of a "mesoscopic-like" behavior in the IS when the sample linear size is of the order of a few times the periodicity of the patterns. It will be interesting if experiments on small samples of type-I superconductors could be performed.

We acknowledge discussions with E. Jagla, M. Meneghini, F. de la Cruz and financial support from ANPCYT, CNEA and Conicet. ADH acknowledges support from CLAF and Fundacion Antorchas.

Present address: The Abdus Salam International Centre for Theoretical Physics, Strada Costiera 11, (34014) Trieste, Italy

- ¹ L.D. Landau, Zh. Eksp. Teor. Fiz. 7, 371 (1937).
- ² R.P. Huebener, Magnetic Flux Structures in Superconductors (Springer-Verlag, New York, 1979).
- ³ R.P. Huebener, R.T. Kamppurth, y V.A. Rowe, Cryogenics 12, 100 (1972).
- ⁴ A. Kienzl and H. Kirschner, J. Low Temp. Phys., 14, 349 (1974).
- ⁵ R.E. Miller and G.D. Cody, Phys. Rev. 173, 494 (1968).
- ⁶ M. Seul and D. Andelman, Science 267, 476 (1995).
- ⁷ H. Castro, B.B. Dutoit, A. Jacquier, M. Baharami, and L.R.inderer, Phys. Rev. B 59, 596 (1999).
- ⁸ C.R. Reisin and S.G. Lipson, Phys. Rev. B 61, 4251 (2000).
- ⁹ V.S. Egorov, G. Solt, C. Baines, D. Herlach, and U. Zimmermann, Phys. Rev. B 64, 024524 (2001).
- ¹⁰ V. Jeudy, C. Gourdou, and T. Okada, Phys. Rev. Lett. 92, 147001 (2004).
- ¹¹ M. Meneghini and R. J. Wijngaarden, preprint.
- ¹² K. Maki, Ann. Phys. 34, 363 (1965); G. Lasher, Phys. Rev. 154, 345 (1967); D.J.E. Callaway, Ann. Phys. 213, 166 (1992).

- ¹³ A. Hubert, Phys. Stat. Sol. 24, 669 (1967).
- ¹⁴ R.N. Goren and M. Tinkham, J. Low Temp. Phys. 5, 465 (1971).
- ¹⁵ E. Fortini and E. Paumier, Phys. Rev. B 14, 55 (1976).
- ¹⁶ J.M. Simolin and A. Lopez, J. Low Temp. Phys. 41, 105 (1980).
- ¹⁷ H. Frahm, S. Ullah, and A.T. Dorsey, Phys. Rev. Lett. 66, 3067 (1991); F. Liu, M. Mondello, and N. Goldenfeld, ibid. 66, 3071 (1991).
- ¹⁸ R.E. Goldstein, D.P. Jackson, and A.T. Dorsey, Phys. Rev. Lett. 76, 3818 (1996); A.T. Dorsey and R.E. Goldstein, Phys. Rev. B 57, 3058 (1998).
- ¹⁹ H. Bokil and O. Narayan, Phys. Rev. B 56, 11195 (1997); O. Narayan, Phys. Rev. Lett. 81, 5035 (1998); R.E. Goldstein and A.T. Dorsey, ibid. 81, 5036 (1998).
- ²⁰ R. Choksi, R.V. Kohn, and F. Otto, J. Nonlinear Sci. 14, 119 (2004).
- ²¹ A.K. Geim, I.V. Goryunova, S.V. Dubonos, J. Lok, J. Maan, A. Filipov, and F. Peeters, Nature 390, 259 (1997).
- ²² E.H. Brandt, Phys. Rev. Lett. 74, 3025 (1995).
- ²³ D. Domnguez and J.V. Jose, Phys. Rev. B 53, 11692 (1996).